Monovalent and Divalent Salt Effects on Electrostatic Free Energies Defined by the Nonlinear Poisson−Boltzmann Equation: Application to DNA Binding Reactions

Shu-wen W. Chen and Barry Honig*

Department of Biochemistry & Molecular Biophysics, Columbia University, 630 W. 168th Street, New York, New York 10032

Received: May 6, 1997; In Final Form: August 19, 1997[⊗]

We have extended the finite-difference Poisson−Boltzmann (FDPB) equation method to incorporate the treatment of mixed salts (i.e. $NaCl/MgCl_2$). In this context, we have derived an expression for the total electrostatic free energy for mixed salt systems. We use the theory to study nonspecific mixed salt effects on the binding free energies of the minor groove binding antibiotic DAPI, and λ repressor, with DNA. We find that in a pure salt solution the electrostatic contribution to binding varies linearly with $\log[M^{n+}]$, (where M^{n+} represents an n-valent cation) and that the effect is uncorrelated with either the valence of the binding ligand or the number of counterions in the binding site. In mixed salt solution, the monovalent and divalent counterions "compete" for the immediate vicinity of the DNA. As experimentally observed in mixed salt solutions, a pronounced curvature appears in the plot of the electrostatic binding free energy vs $\log[M^{n+}]$. The curvature for DAPI−DNA binding in mixed salts reflects the fact that divalent counterions interact with bound or free DNA molecules more strongly than monovalent counterions. However, the valence dependence of the electrostatic interaction between cations and negatively charged macromolecules is not solely responsible for the observed curvature. Rather anions, which can interact quite strongly with highly charged DNA-binding proteins, make a significant contribution to the observed salt effects. Our results support previous findings that treatments based on counterion condensation concepts break down for protein−DNA interactions; specifically, it is necessary to describe molecular structures in atomic detail if a realistic description of salt effects is to be obtained.

I. Introduction

The ionic environment is a crucial determinant of the structure and function of biologically active macromolecules;[1−4] in particular, salt concentration is known to have a strong effect on the binding free energies of various drugs [5,6] and proteins[7,8] to DNA. It is known, for example, that different operator binding sites can be differentiated by the salt dependence of the binding constant with the same repressor.[7] These salt effects have been extensively studied both experimentally and theoretically and have been described in terms of the dependence of binding constants[9,10] (or electrostatic binding free energies[6,8,11−13]) on the salt concentration in solution.

Counterion condensation (CC) theory has been widely used to study salt effects on nucleic acids.[14,15] CC theory has been remarkably successful in its ability to reproduce experimental data for nonspecific salt effects on ligand−DNA binding in pure and mixed salt solutions.[15−17] However, the fact that CC theory does not incorporate an atomic level description of molecular structure limits its ability to describe many electrostatic features of complex biological macromolecules.[18] In addition, it has been pointed out that CC theory cannot account for the observed salt dependence of both the enthalpy and entropy of binding.[6,8] One alternative is provided by Monte Carlo simulations, which have been used primarily to study model systems (i.e. cylindrical DNA models[19,20]) but have also been applied to the study of λcI repressor−DNA interactions.[21] Such simulations can be of great value, but they are computationally quite demanding.

Numerical solutions to the nonlinear Poisson−Boltzmann equation (NLPB) have been shown to accurately account for nonspecific salt effects on electrostatic interactions involving DNA.[6,8,22,23] A solvation formalism has been developed within the context of the NLPB equation that makes it possible to evaluate thermodynamic contributions to ligand−DNA binding free energies for 1−1 salt solutions.[24] In this work we extend this theory to mixed salt systems and apply it to describe the interactions of complex molecules described in atomic detail. Previous applications of the NLPB equation to mixed salt solutions have been limited to simple geometric models of polyions.[13,25,26] A preliminary study of mixed salt effects on ligand−DNA binding free energies has been reported previously.[11]

Following the procedure developed previously for 1−1 salt solutions,[24] in this work we obtain an expression for the total electrostatic free energy of a system containing a mixture of 1−1 and 2−1 salts. (For clarity of presentation, we will assume that we are dealing with a mixture of NaCl and $MgCl_2$.) The spatial dependence of the population of each ionic species is described by a Boltzmann factor governed by the electric potentials that are salt dependent.[27] Numerical calculations of binding free energies in both pure and mixed salts solutions are carried out for both the DAPI−DNA[28] and λcI repressor−DNA[29] complex. The results we obtain allow us to examine the role of molecular charge distribution on the salt dependence of the binding process and to describe the nature of the competition between monovalent and divalent ions for the immediate vicinity of highly charged macromolecules.

Our results provide new insights as to the relative effects of monovalent and divalent ions on the properties of highly charged macromolecules such as nucleic acids. In addition, by providing a complete description at the level of the NLPB equation of nonspecific ion effects, they should facilitate the identification of cases where it is necessary to invoke the binding of ions to specific sites on the surface of macromolecules in order to account for experimental observations.

[⊗] Abstract published in *Advance ACS Abstracts,* October 1, 1997.

S1089-5647(97)01521-6 CCC: $14.00

II. Methods

A. The Total Electrostatic Free Energy. We begin by deriving the PB equation for mixed salt solutions. The Poisson equation is given by

$$\nabla\cdot[\epsilon(r)\nabla\psi(r)] + 4\pi\rho(r) = 0 \tag{1}$$

where $\psi(r)$ is the electrostatic potential at r, $\epsilon(r)$ is the spatially varying dielectric constant, and $\rho(r)$ is the charge density. For systems containing fixed charges on the solute and mobile ions, the charge density can be written as the sum

$$\rho(r) = \rho_f(r) + \rho_m(r) \tag{2}$$

where $\rho_f(r)$ is the charge density of the solute and $\rho_m(r)$ is that of the mobile ions.

The charge density of mobile ions in the NLPB model is evaluated according to Boltzmann statistics as a sum of contributions from all the ionic species in solution. That is

$$\rho_m(r) = \sum_i c_i^{bulk} Z_i e_o \exp\left(\frac{-Z_i e_o \psi(r)}{k_B T}\right) \tag{3}$$

where c_i^{bulk} is the bulk concentration of ionic species i, Z_i is the valence of i, and e_o is the unit of protonic charge, k_B is the Boltzmann constant, and T is the temperature. For a system containing NaCl and $MgCl_2$, $\rho_m(r)$ can be explicitly expressed as

$$\rho_m(r) = c_{Na}^{bulk} e_o\left[Z_{Na}\exp\left(\frac{-Z_{Na}e_o\psi(r)}{k_B T}\right) + Z_{Cl}\times \exp\left(\frac{-Z_{Cl}e_o\psi(r)}{k_B T}\right)\right] + c_{Mg}^{bulk} e_o\left[Z_{Mg}\exp\left(\frac{-Z_{Mg}e_o\psi(r)}{k_B T}\right) + 2Z_{Cl}\exp\left(\frac{-Z_{Cl}e_o\psi(r)}{k_B T}\right)\right] \tag{4}$$

Defining the ionic strength of solution, $I = I_{Na} + I_{Mg}$, the bulk concentrations of 1−1 and 2−1 salts in the above equation can be replaced by I_{Na} and I_{Mg} with the following relations: $I_{Na} = c_{Na}^{bulk}$ and $I_{Mg} = 3c_{Mg}^{bulk}$. The NLPB equation can now be written in the form

$$\nabla\cdot[\epsilon(r)\nabla\phi(r)] + f(\phi(r)) = 0 \tag{5}$$

where

$$f(\phi(r)) = \frac{4\pi e_o}{k_B T}\rho_f(r) + \frac{4\pi e_o}{k_B T}\left\{-2I_{Na}e_o\sinh(\phi(r)) - \frac{2}{3}I_{Mg}e_o[\exp(\phi(r)) - \exp(-2\phi(r))]\right\} \tag{6}$$

where $\phi(r) = \psi(r)/k_B T$ is the reduced electric potential. The total electrostatic free energy, G^{el}, is a functional of electrostatic potentials and can be expressed as[24]

$$G^{el} = \int F(\phi(r),\nabla\phi(r);r)\,dr \tag{7}$$

For convenience we define $\kappa_{Na}^2 = 8\pi e_o^2 I_{Na}/\epsilon k_B T$ and $\kappa_{Mg}^2 = 8\pi e_o^2 I_{Mg}/\epsilon k_B T$ where each κ can be viewed as a Debye−Hückel screening parameter specific to a particular ion.[27] Following Sharp and Honig,[24] we use the Euler−Lagrange undetermined multipliers method and a variational principle to find the general form, $C_1F + C_0$, of the energy density function $F(\phi(r),\nabla\phi(r);r)$. C_1 is set to $1/4\pi$ so as to conform to the usual electrostatic convention, while the fact that $G^{el} = 0$ when $\phi(r) = 0$ everywhere requires that $C_0 = \epsilon\kappa_{Na}^2/4\pi + \epsilon\kappa_{Mg}^2/8\pi$. It is now straightforward to show that

$$G^{el} = \int\left\{\rho_f(r)\,\psi(r) - k_B T c_{Na}^{bulk}(2\cosh(\phi(r)) - 2) - k_B T c_{Mg}^{bulk}\times [2\exp(\phi(r)) + \exp(-2\phi(r)) - 3] - \frac{\epsilon}{8\pi}\left|\nabla\psi(r)\right|^2\right\}dr \tag{8}$$

It is worth pointing out that the third, c_{Mg}, dependent, term in eq 8 corresponds to the excess osmotic pressure for the divalent salt. (Equation 8 is the mixed-salt analogue of eq 13 in ref 24.) To study nonspecific salt effects on intermolecular binding, we define the salt-dependent electrostatic binding free energy as[6]

$$\Delta\Delta G_s^{el} = \Delta G_{cmp}^{el} - \Delta G_{DNA}^{el} - \Delta G_{lig}^{el} \tag{9}$$

where lig denotes the free ligand, DNA is the free DNA molecule, and cmp is the bound complex. The Δ's on the right-hand side of the above equation indicate a difference between the electrostatic free energy of the system at a given salt concentration and the electrostatic free energy of the system in a pure solvent.

The salt dependence of the binding free energy, $m_{bind} = -\partial\log(K_{obs})/\partial\log[M^{n+}]$, is given by[6]

$$m_{bind} = \frac{\partial(\Delta\Delta G_s^{el})}{\partial(\log[M^{n+}])} \tag{10}$$

where $[M^{n+}]$ is the salt concentration of n^+ valent counterions. $\Delta\Delta G_s^{el}$ is in units of $2.3k_B T$. In this paper the value of m_{bind} is obtained from a linear least-squares fit of plots of $\Delta\Delta G_s^{el}$ vs log $[M^{n+}]$ shown in the various figures (the 1 M and 2 mM points were excluded from the fits). Since the plots are not completely linear, the values of m_{bind} obtained in this paper are an average over a wide range of salt concentrations and do not correspond to the slope at a particular point. Alternatively, as shown in ref 13 (see eq 10) , m_{bind} at a particular point can be obtained directly from the excess ion concentration of the salt whose concentration is being varied. We have verified (results not shown) that the two methods give similar results. On the basis of eq 9, we can identify three specific components of m_{bind}:

$$m_{bind} = \frac{\partial(\Delta G_{cmp}^{el})}{\partial(\log[M^{n+}])} - \frac{\partial(\Delta G_{DNA}^{el})}{\partial(\log[M^{n+}])} - \frac{\partial(\Delta G_{lig}^{el})}{\partial(\log[M^{n+}])} = m_{cmp} - m_{DNA} - m_{lig} \tag{11}$$

B. Numerical Implementation. The numerical algorithm used to obtain finite-difference solutions to the NLPB equation has been described elsewhere.[30−32] Space is divided into an $N \times N \times N$ grid points ($N = 65$ in this work). Using Gauss's theorem, a surface integral form of the NLPB equation[32] for a mixed salt system can be written as

$$\int\epsilon\nabla\phi(r)\cdot dS - \tilde\kappa_{Na}^2\sinh(\phi(r))h^3 - \tilde\kappa_{Mg}^2[\exp(\phi(r)) - \exp(-2\phi(r))]h^3 + \frac{4\pi e_o}{k_B T}\int\rho_f(r)\,dr = 0 \tag{12}$$

where reduced Debye−Hückel parameters $\tilde\kappa_{Na}^2$ and $\tilde\kappa_{Mg}^2$ are defined as $\epsilon\tilde\kappa_{Na}^2$ and $^1/_3\epsilon\kappa_{Mg}^2$ respectively, and h is the grid spacing.

Numerically, the solution of the NLPB equation, ϕ_o, at the grid point o can be obtained from

$$\phi_o = \frac{\sum_{i=1}\epsilon_i\phi_i + \frac{4\pi q_o}{h}}{(\mathrm{LN} + \mathrm{NLN})} \quad (13)$$

where ϕ_i is the electric potential at one of the six grid points, i, surrounding the point o.

$$\mathrm{LN} = \sum_i \epsilon_i + (\tilde{\kappa}^2_{\mathrm{Na,o}} + 3\tilde{\kappa}^2_{\mathrm{Mg,o}})h^2 \quad (14)$$

and

$$\mathrm{NLN} = \sum_n \left\{ \tilde{\kappa}^2_{\mathrm{Na,o}} \frac{\phi_o^{2n}}{(2n+1)!} + \tilde{\kappa}^2_{\mathrm{Mg,o}} \left[\frac{\phi_o^n}{(n+1)!}(1 - (-2)^{n+1}) \right] \right\} \quad (15)$$

The infinite series over n defined in Equation 15 was terminated after $n = 3$. $\tilde{\kappa}^2_{\mathrm{Na,o}}$ and $\tilde{\kappa}^2_{\mathrm{Mg,o}}$ are the corresponding reduced Debye−Hückel parameters at the grid point o and ϵ_i is the assigned dielectric constant between the points i and o. If the NLN term is omitted from eq 13, one obtains the linearized version of the PB equation for mixed salt systems.

The assignment of charges and other quantities to grid points is described elsewhere.[32] We used a three-step focusing procedure to improve the precision of the results.[30] Boundary electric potentials in every step are obtained from linear interpolation of electric potentials calculated in the previous step. Boundary electric potentials in the first step are obtained by applying the Debye−Huckel expression to a single positive and single negative charge whose magnitudes are equal to the net positive and negative charge, respectively, and which are located at the center of positive and negative charge, respectively. In the three focusing steps, the solutes occupy 23%, 46%, and 92% of the volume of the cubic box, respectively.

C. Molecular Models. We assume that the molecules undergo no conformational change as a consequence of the association process so that the coordinates of the uncomplexed molecules are assumed to be identical with those of the complex. Coordinates for 4′-6-diamidine-2-phenylindole (DAPI) complexed with the B-form oligonucleotide, C-G-C-G-A-A-T-T-C-G-C-G were taken form Larsem et al.[28] Hydrogen atoms were added to the heavy atoms in the structure with the DISCOVER program.[33] Partial charges and radii of atoms are from the CVFF force field.[34]

Coordinates for the λcI repressor complex with the O_L1 operator site were obtained from the study of Beamer et al.[29] O_L1 consists of 20 base pairs with the sequence A-A-T-A-C-C-A-C-T-G-G-C-G-G-T-G-A-T-A-T. Coordinates of the first five residues in the monomer bound to the nonconsensus half-site of DNA are missing in X-ray crystal structure. These were built from the corresponding residues in the other monomer as described previously.[8] Hydrogen atoms were added to the structure as described for the DAPI−DNA complex.

All regions inside the molecular surface are assigned a dielectric constant of 2, and water is assigned a dielectric constant of 80. An ion exclusion radius of 2.0 Å was used for all ions.

III. Results and Discussion

A. DAPI−DNA Interactions. (1) *Pure Salt Effects*. The electrostatic contribution to the binding free energy, $\Delta\Delta G^{\mathrm{el}}_s$, is plotted in Figure 1 as a function of salt concentration. As has been found in previous studies $\Delta\Delta G^{\mathrm{el}}_s$ is greater than zero and increases linearly with log[salt]. The three components, $m_{\mathrm{bind}} - m_{\mathrm{cmp}}$, m_{DNA}, and m_{lig}, are listed in Table 1. That all three are negative is simply an indication that each molecule (or complex) interacts favorably with its own ion atmosphere. The larger the slope, the more pronounced the salt dependence, which, for the DAPI−DNA complex, is strongly correlated with the net charge on the solute. In contrast to its components, m_{bind} is found to be greater than zero with values of 2.36 and 1.49 for NaCl and $MgCl_2$ salts, respectively. As has been noted in previous work,[6] the former number is in good agreement with experiment (to our knowledge, the dependence of DAPI binding on divalent ion concentration has not been measured). At high enough salt concentrations, the ion atmosphere around a particular solute becomes increasingly saturated for both Na^+ and Mg^{2+}, and as a result, the sensitivity of the electrostatic free energy to the valence of counterions is reduced. In contrast to its components, m_{bind} has a positive sign, which implies that salt opposes binding.

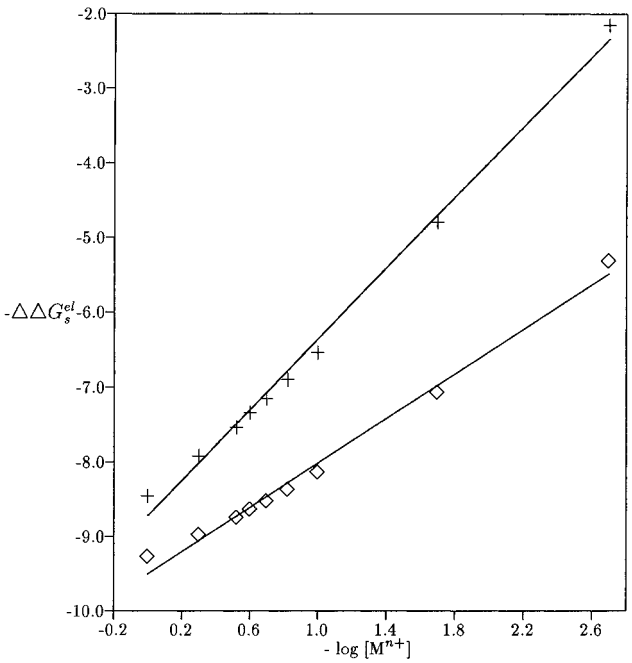

Figure 1. Salt dependent electrostatic binding free energy of the DAPI-DNA complex in 1−1 and 2−1 salts. +: 1−1 salts; ◇: 2−1 salts. The solid lines represent linear least-squares fits of the calculated data.

TABLE 1: Salt Dependence of Various Free Energy Values for DAPI-DNA and λCI Repressor−DNA Binding in Pure Salt Solution

salt	m_{cmp}	m_{DNA}	m_{lig}	m_{bind}
1−1[a]	−9.54	−11.71	−0.19	2.36
2−1[a]	−6.56	−7.84	−0.21	1.49
1−1[b]	−22.34	−22.22	−4.00	3.89
2−1[b]	−13.98	−12.65	−4.58	3.26

[a] DAPI−DNA binding. [b] λcI repressor−DNA binding.

As seen in Figure 1, the electrostatic binding free energy at the same concentration is more unfavorable in $MgCl_2$ than in NaCl. This is because the removal of divalent ions from the vicinity of DNA is more costly energetically than the removal of monovalent ions. At high salt concentration, the difference between the binding free energies in the two salt solutions is reduced as the ion atmosphere around the DNA becomes saturated in either solution. The interaction of DAPI with anions is quite small as indicated by the small value of m_{lig}. Consequently, m_{bind} is determined primarily by the difference in the

values of m_{DNA} and m_{cmp}, which is due primarily to the neutralization of charge on the DNA by the binding of DAPI. That m_{DNA} and m_{cmp} in $MgCl_2$ are less negative than the comparable values in NaCl (Table 1) may seem counterintuitive since one expects the interaction of DNA to be weaker with monovalent ions than with divalent ions. However recalling (eq 10 in ref 13) that the various slopes correspond to the excess number of ions around a solute molecule and that the anions make a small contribution to m_{cmp} for DAPI, the smaller slope for Mg can be simply understood as resulting from the fact that fewer divalent than monovalent ions accumulate around DNA. Consequently, the electrostatic free energy of the polyion is less sensitive to variations in divalent ion concentration than monovalent ion concentration.

(2) Mixed Salt Effects. Figure 2a plots the electrostatic binding free energy vs log [cation] for a 1−1 salt in the presence of a 2−1 salt. As is evident from Figure 2a, in mixed salts the binding free energy plots are no longer linear with the curvature increasing with increasing divalent ion concentration. The calculated curvature may be understood in terms of the differential interactions of monovalent and divalent cations with DNA. Since divalent ions interact more strongly with DNA and hence have a stronger tendency to accumulate in its vicinity,[25,35] the interaction between DNA and monovalent ions will be screened by the divalent ions, thus reducing the sensitivity of binding to monovalent ion concentration. This explains why at low monovalent concentrations, the slope of the curves in Figure 2a tends to be flat. At higher monovalent ion concentrations, the monovalents increasingly accumulate in the vicinity of DNA and consequently have an increasingly large effect on the binding free energy. Indeed as the concentration of monovalent ions increases, the electrostatic binding free energy approaches the value for pure 1−1 salts.

Figure 2b plots the electrostatic binding free energy vs log [cation] for a 2−1 salt in the presence of a 1−1 salt. In contrast to Figure 2a, essentially no curvature is observed in the plots. This simply reflects the greater tendency of divalent ions to accumulate in the vicinity of DNA so that the effect of monovalent ions is greatly reduced. Overall, the observed curvature may be understood in terms of a competition between monovalent and divalent ions, not for a specific site on the surface of DNA but rather for its general vicinity.

B. λcI Repressor−O_L1 Interactions. *(1) Pure Salt Effects*. As shown in Figure 3, the calculated electrostatic binding free energy of the λcI repressor−O_L1 complex is linearly correlated with log [salt]. m_{bind} is calculated to be 3.89 and 3.29 in pure NaCl and $MgCl_2$, respectively. The former value has been obtained previously and is in good agreement with experiment.[8] In contrast to the case for DAPI, the values of m_{bind} for the λcI repressor−O_L1 complex in 1−1 and 2−1 salts are quite similar. m_{cmp}, m_{DNA}, and m_{lig} are more negative than for DAPI binding, reflecting in part the longer oligomer present in the repressor complex for the first two values. In contrast to DAPI, the value of m_{lig} for the λcI repressor is significant even though its net charge is identical with that of DAPI. The larger value for the protein is due to its complex charge distribution, which allows many charged sites to interact individually with the ion atmosphere. Given the presence of many basic groups on the protein, anions clearly play an important role in the net electrostatic interaction with the ion atmosphere.

As is the case for DAPI, the absolute values of m_{cmp} and m_{DNA} for the λcI repressor−DNA complex are larger in 1−1 salts than in 2−1 salts. However in contrast to the DAPI complex, m_{cmp} is greater than that of m_{DNA} and is significantly more negative in the 2−1 salt. For the DAPI complex, the

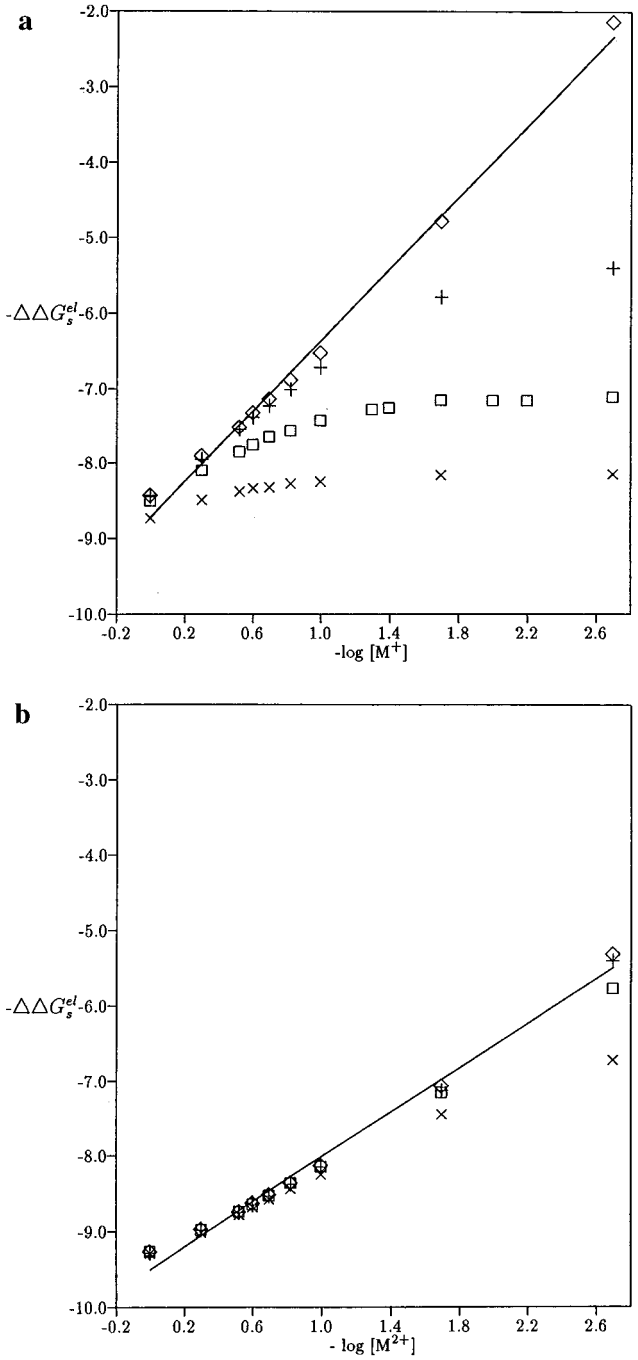

Figure 2. Electrostatic binding free energy of the DAPI−DNA complex as a function of log [cation]. (a) Plotted as a function of log [M^+] in the presence of a 2−1 salt: (◇) [M^{2+}] = 0.0 M; (+) [M^{2+}] = 0.002 M; (□) [M^{2+}] = 0.02 M; (×) [M^{2+}] = 0.1 M. The solid line in the figure is the linear least-squares fit of the data in a pure 1−1 salt. (b) Plotted as a function of log [M^{2+}] in the presence of a 1−1 salt: (◇) [M^+] = 0.0 M; (+) [M^+] = 0.002 M; (□) [M^+] = 0.02 M; (×) [M^+] = 0.1 M. The solid line is the linear least-squares fit of the data in pure 2−1 salts.

difference between m_{cmp} and m_{DNA} is a consequence of charge neutralization in the DNA due to DAPI binding. However even though charge neutralization takes place in the λcI repressor complex as well, the distributed charge distribution of the complex involving both positive and negative charges causes it to be more sensitive to the ion atmosphere (both to anions and cations) than the isolated DNA molecule. Thus, both anions and cations are responsible for the value of m_{cmp} as they are for m_{lig}. Since m_{bind} is a result of the composite salt effects of all ionic species in solution, its value is a sensitive function of

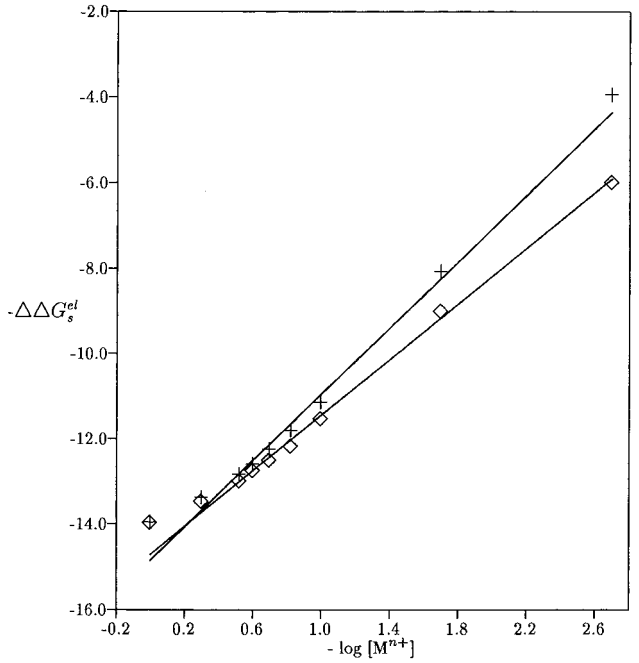

Figure 3. Salt dependent electrostatic binding free energy of the λcI repressor−DNA complex in 1−1 and 2−1 salts: (+) 1−1 salts; (◇) 2−1 salts. The solid lines are the linear least-squares fits of the relevant data.

the charge distribution of the interacting molecules but not of the valence of the binding ligand. Clearly, simple CC-based concepts break down for protein DNA interactions as has been found previously.

(2) Mixed Salt Effects. Figure 4a plots $\Delta\Delta G_s^{el}$ vs log [NaCl] for λcI repressor−DNA binding. As was found for DAPI−DNA binding (Figure 2a), there is a pronounced curvature in the plots in mixed salt solution which is increased with increasing $MgCl_2$ salt concentration. Figure 4b plots $\Delta\Delta G_s^{el}$ vs log [$MgCl_2$] in the presence of NaCl. Here, in contrast to the case of DAPI binding (Figure 2b), the presence of NaCl is found to have a significant effect on the calculated plots. The difference between DAPI and the λcI repressor must be due to Cl^- ion effects since the competition between monovalent and divalent cations must be similar in both systems. Indeed it is evident from Table 1 that much of the contribution to m_{bind} for the repressor is due to m_{lig}, which is strongly dependent on Cl^- concentration. At low [$MgCl_2$], the presence of NaCl provides the Cl^- ions that interact with the protein and thus reduce the sensitivity of the binding free energy to [$MgCl_2$]. At higher [$MgCl_2$] or lower [NaCl], the effects of Cl^- ions are largely due to the $MgCl_2$ leading to a greater sensitivity to the concentration of this salt.

Although the necessary data are not available to allow a direct comparison with experiment for λcI repressor−DNA interactions, we note that significant curvature has been observed in plots of the NaCl dependence of *lac*-repressor-DNA binding in the presence of $MgCl_2$.[36] Although this has been attributed to a competition between Mg^{2+} ions and the protein for DNA,[36] the results presented here demonstrate that significant curvature is a direct consequence of the NLPB equation, thus providing a straightforward explanation of the observed salt dependence of the binding free energies.

IV. Conclusions

In this paper we have used the NLPB as a basis for describing the effects of monovalent and divalent ions in pure and mixed salt solutions on the binding of ligands and proteins to DNA.

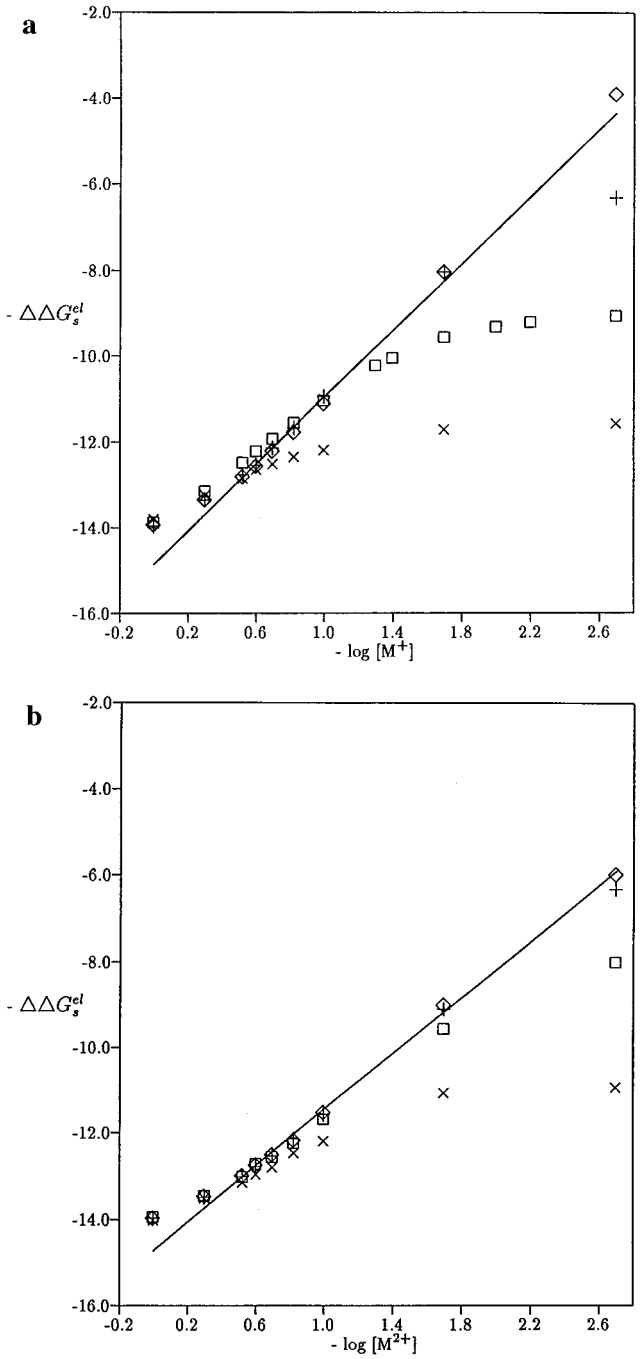

Figure 4. Electrostatic binding free energy of the λcI repressor−DNA complex as a function of log [cation]. (a) Plotted as a function of log [M^+] in the presence of a 2−1 salt: (◇) [M^{2+}] = 0.0 M; (+) [M^{2+}] = 0.002 M; (□) [M^{2+}] = 0.02 M; (×) [M^{2+}] = 0.1 M. The solid line in the figure is the linear least-squares fit of the data in a pure 1−1 salt. (b) Plotted as a function of log [M^{2+}] in the presence of a 1−1 salt: (◇) [M^+] = 0.0 M; (+) [M^+] = 0.002 M; (□) [M^+] = 0.02 M; (×) [M^+] = 0.1 M. The solid line corresponds to the linear least-squares fit of the data in a pure 2−1 salt.

The methodology in the paper is quite general and can be applied to a variety of other problems involving valence specific effects on nucleic acid structure and function, for example, nonspecific Mg^{2+} effects on RNA folding.

In previous work we have discussed the fact that the NLPB approach yields insights as to the nature of salt effects on the binding process that are rather different than those offered by CC-based models.[6,8,11−13] With regard to the current work, one of the most important findings has been the importance of anion−protein interactions on the overall salt dependence of the binding process. In addition this work emphasizes the need

to treat molecular structures in atomic detail if a realistic description of the salt dependence is to be obtained.

With regard to mixed salt effects, our work highlights the competition between monovalent and divalent ions for the vicinity of a highly charged polyelectrolyte and demonstrates that curvature in plots that relate binding free energy to log [salt] is a natural consequence of this competition. This suggests that competitive binding models that have at times been invoked to explain the curvature observed in the salt dependence of protein binding to DNA may be unnecessary; rather curvature appears due to nonspecific effects to the inherent nature of the ion atmosphere.

Acknowledgment. This work was support by NIH Grant GM -41371. We also thank Drs. Jonathan L. Hecht and Jean-Luc Pellequer for many useful conversations and help with the calculations. Professor Kim Sharp is gratefully acknowledged for his many helpful comments on the manuscript.

References and Notes

(1) Rich, A.; Seeman, N.; Rosenberg, J. *Nucleic Acid−Protein Recognition*; Academic: New York, 1977.
(2) Drew, H.; Takano, T.; Tanaka, S.; Ikatura, K.; Dickerson, R. *Nature* **1980**, *286*, 567.
(3) Mitra, C.; Sarma, M.; Sarma, R. *J. Am. Chem. Soc.* **1981**, *103*, 6727.
(4) Bacquet, R.; McCammon, J. *J. Phys. Chem.* **1988**, *92*, 7134.
(5) Wilson, W.; Tanious, F.; Barton, H.; Jones, R.; Fox, K.; Wydra, R.; Strekowski, L. *Biochemistry* **1990**, *29*, 8452.
(6) Misra, V.; Sharp, K.; Friedman, R.; Honig, B. *J. Mol. Biol.* **1994**, *238*, 245.
(7) Senear, D.; Batey, R. *Biochemistry* **1991**, *30*, 6677.
(8) Misra, V.; Hecht, J.; Sharp, K.; Friedman, R.; Honig, B. *J. Mol. Biol.* **1994**, *238*, 264.
(9) Lohman, T.; deHaseth, P.; Record, T., Jr. *Biochemistry* **1980**, *19*, 3522.
(10) deHaseth, P.; Lohman, T.; Record, T., Jr. *Biochemistry* **1977**, *16*, 4783.
(11) Chen, S.-w.; Honig, B. *Biophys. J.* **1994**, *66*, A291.
(12) Sharp, K.; Friedman, R.; Misra, V.; Hecht, J.; Honig, B. *Biopolymers* **1995**, *36*, 245−262.
(13) Sharp, K. *Biopolymers* **1995**, *36*, 227−243.
(14) Manning, G. *J. Chem. Phys.* **1969**, *51*, 3249.
(15) Manning, G. *Q. Rev. Biophys. II* **1978**, *2*, 179.
(16) Record, M., Jr; Anderson, C.; Lohman, T. *Q. Rev. Biophys. II* **1978**, *2*, 103.
(17) Record, M., Jr; Lohman, T.; DeHaseth, P. *J. Mol. Biol.* **1976**, *107*, 145.
(18) Gueron, M.; Weisbuch, G. *Biopolymers* **1980**, *19*, 353.
(19) Olmsted, M. C.; Bond, J. P.; Anderson, C. F.; Record, T., Jr. *Biophys. J.* **1995**, *68*, 634−647.
(20) Mills, P. *Biophys. J.* **1995**, *68*, 400−401.
(21) Jayaram, B.; DiCapua, F.; Beveridge, D. *J. Am. Chem. Soc.* **1991**, *113*, 5211.
(22) Hecht, J. L.; Honig, B.; Shin, Y.; Hubbell, W. *J. Phys. Chem.* **1995**, *99*, 7782−7786.
(23) Misra, V.; Honig, B. *Proc. Natl. Acad. Sci. U.S.A.* **1995**, *92*, 4691−4695.
(24) Sharp, K.; Honig, B. *J. Phys. Chem.* **1990**, *94*, 7684.
(25) Ramanathan, G. *J. Chem. Phys.* **1986**, *85*, 2957.
(26) Weisbuch, G.; Gueron, M. *J. Phys. Chem.* **1981**, *85*, 517.
(27) McQuarrie, D. *Statistical Mechanics*; Harper & Row: New York, 1976.
(28) Larsem, T.; Goodsell, D.; Cascio, D.; Grzeskowiak, K.; Dickerson, R. *J. Biomol. Struct. Dyn.* **1989**, *7*, 477.
(29) Beamer, L.; Pabo, C. *J. Mol. Biol.* **1992**, *227*, 177.
(30) Gilson, M.; Sharp, K.; Honig, B. *J. Comput. Chem.* **1988**, *9*, 327.
(31) Sharp, K.; Honig, B. *Chem. Scr.* **1989**, *29A*, 71.
(32) Klapper, I.; Hagstrom, R.; Fine, R.; Sharp, K.; Honig, B. *Proteins* **1986**, *1*, 47.
(33) Biosym. Discover, 3.1 ed.; Biosym Technologies, Inc: San Diego, CA, 1993.
(34) Hagler, A.; Stern, P.; Sharon, R.; Becker, J.; Naider, F. *J. Am. Chem. Soc.* **1979**, *101*, 6842.
(35) Murthy, C.; Bacquet, R.; Rossky, P. *J. Phys. Chem.* **1985**, *89*, 701.
(36) Record, M., Jr; DeHaseth, P.; Lohman, T. *Biochemistry* **1977**, *16*, 4791.